Available online at www.sciencedirect.com
SCIENCE DIRECT®
Journal of Membrane Science 279 (2006) 608–614
journal of MEMBRANE SCIENCE
www.elsevier.com/locate/memsci

Direct measurement of nanofluxes and structural relaxations of perfluorinated ionomer membranes by scanning probe microscopy

Joseph H. Wei [a], Mingyan He [b], René M. Overney [a,*]

[a] *Department of Chemical Engineering, University of Washington, Box 351750, Seattle, WA 98195, United States*
[b] *Department of Chemistry, University of Washington, Box 351700, Seattle, WA 98195, United States*

Received 3 September 2005; received in revised form 22 November 2005; accepted 24 December 2005
Available online 3 February 2006

Abstract

This nanorheological study addresses the water transport hindrance in perfluorinated ionomer membranes (Nafion® H^+ form) in conjunction with structural relaxation properties of the polymer matrix. A low-temperature relaxation of the "dry" Nafion® matrix at 79 °C, about 35 °C below the glass transition temperature, was found to be responsible for a steady improvement of the water transport above 70 °C. The low-temperature structural transition at 79 °C was observed for the dehydrated membrane, and thus, is specific to the polymer matrix and not a sole consequence of the kinetics of the solvent-containing aggregates within the apolar perfluorocarbon matrix. Water was found to be trapped within a hydrated perfluorinated ionomer membrane below 70 °C. The direct observation of water transport is possible with a novel scanning force microscopy (SFM) method, flux-lateral force microscopy (F-LFM). With this technique, local fluid permeation fluxes are directly obtained at the membrane downstream surface. The structural transition properties were acquired by another highly sensitive nanoscopic technique, shear modulation force microscopy (SM-FM).

Keywords: Permeation; Nafion®; Glass transition; Atomic force microscopy; Nanoflux

1. Introduction

To date, the most widely used polymer electrolyte membrane (PEM) material in fuel cell application is Nafion®, an ionic copolymer (ionomer). It consists of a poly(tetrafluoroethylene) backbone with short perfluoro-polyether pendant side chains terminated by ionizable sulfonate groups. When swollen in a polar solvent (water or alcohols), a complex organized structure is responsible for excellent ionic conductivity and electrochemical and chemical resistance [1,2]. Our current understanding of the Nafion® structure is that it resembles a three-dimensional array of inverse micelles that are interconnected by short channels acting as transient crosslinks [3]. The micelles, 30–50 Å in size, consist of ionic end groups from the side chains that are clustered together in solvent-containing aggregates within the apolar perfluorocarbon matrix [1].

Nafion® membranes are rigid systems with poor proton conduction unless a polar solvent is absorbed. For insufficiently hydrated Nafion® membranes, the proton transport is slow, and thus, the conversion efficiency negatively affected [4]. On the other hand, excess water can lead to cathode flooding in the system, resulting in a reduced efficiency [5]. Good water management usually requires balancing the electro-osmotic drag and diffusion of water [6,7]. It has been realized that the microstructural properties of the membrane are very important in explaining solvent swelling [8,9].

Besides water transport, the gas permeability, particularly of oxygen and hydrogen, is of significance for an effective PEM membrane operation. Originally, it was argued that the gas mainly permeates either through the hydrated ionic cluster region [10], or through the hydrophobic amorphous region of the membrane [11]. However, recent experiments have shown that both regions have to be considered for gas transport [12].

Considering the complexity of Nafion® intertwines a rheological polymer cluster network with the intricacy of solvent swelling and ionic conductivity, it would be desirable to

* Corresponding author. Tel.: +1 206 543 4353; fax: +1 206 543 3778.
E-mail address: roverney@u.washington.edu (R.M. Overney).

0376-7388/$ – see front matter © 2006 Elsevier B.V. All rights reserved.
doi:10.1016/j.memsci.2005.12.055

investigate gas transport and swelling in conjunction with the rheological relaxation properties of the polymer matrix. In the late 1970s and 1980s, Eisenberg and coworkers devoted great efforts towards a proper determination of the rheological properties of Nafion® on a macroscopic level with indications of a likely structural relaxation tens of degrees below the glass transition temperature [1,13–15]. In 1995, Sen et al. argued the possibility of a structural change within Nafion® around 80–90 °C based on a viscosity curve analysis [16]. Over the past decades, the main focus has been on the solvent swollen membrane. Early on, Riecke and Vanderborgh found that a decrease in resistivity around 80–90 °C is due to a reduction in the activation barriers for proton motion, i.e., interpreted their results with the availability of water to ionize the sulfonic acid groups [17]. However, the fundamental question still remained: what makes water flow, or restricts its flow through the membrane?

With this paper, we address the combined effect of Nafion's® water transport ability and its structural polymer matrix relaxations below the glass transition. Shear modulation force microscopy (SM-FM) [18], a scanning force microscopy (SFM) mode, was used to investigate the possibility of rheological transitions at low temperatures of Nafion®. Local mass transport was studied with flux-lateral force microscopy (F-LFM), a novel SFM mode. The introduction of a microscopic method to the mass transport analysis in PEM fuel cells is motivated by current miniaturization trends in PEM technology involving interfacially confined polymer matrices [19]. Spatial confinement, as shown for ultrathin films, can invoke changes in the polymer relaxation dynamics [18,20–23] and consequently lead to alterations of transport properties.

2. Experimental

2.1. Materials

Highly purified Nafion® was used for structural relaxation analysis involving SM-FM, Fig. 1, to avoid surface contamination of low molecular weight materials, as SM-FM is a highly sensitive surface contact mechanical method. The Nafion® film was spin cast from a Nafion® perfluorinated ion-exchange resin (Product number 274704, Sigma–Aldrich Inc.) onto a silicon (1,1,1)-oriented wafer (Mitsubishi Silicon America) at 53.58 Hz (3215 rpm) with a spin coater (P6204, Specialty Coating Systems) and annealed at 135 °C for 65 min under vacuum (VWR brand). Prior to spin casting, the silicon wafer was sequentially rinsed with acetone (15 min), methanol (30 min) and DI water. The Nafion® perfluorinated ion-exchange resin (H^+ form) contained 5 wt.% solution in a mixture of lower aliphatic alcohols and water (20%), with an equivalent weight (EW) of 1100 [24]. The Nafion® film thickness was 241 ± 2 nm determined by profilometry (KLA Tensor Alpha-Step 500).

The sample, investigated with F-LFM concerning its water transport behavior, was a commercial Nafion® 115 membrane (EW of 1100, FuelCellStore.com, Boulder, CO), chosen to be as close as possible to a conventional membrane electron assembly (MEA) in an actual PEM fuel cell device. The membrane was glued with a 5 min epoxy gel (*ITW* Devcon) on a custom-made copper ring with an inner diameter of 0.254 cm (0.1 in.) and an outer diameter of 2.54 cm (1 in.) that fits into the F-LFM membrane chamber, Fig. 2. Prior to gluing, the copper ring surface was roughened with a scalpel to enhance the strength of the Nafion®–epoxy–copper interface and to prevent delamination of

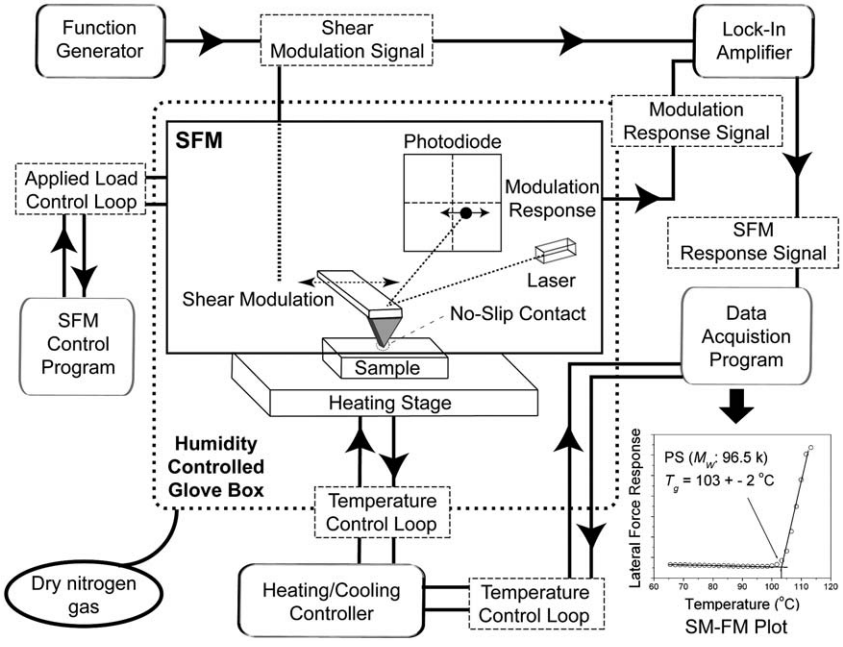

Fig. 1. Illustration and schematic of the SM-FM set-up. A representative SM-FM plot of polystyrene is shown at bottom right. The glass transition temperature, T_g, is identified by the kink in the plot.

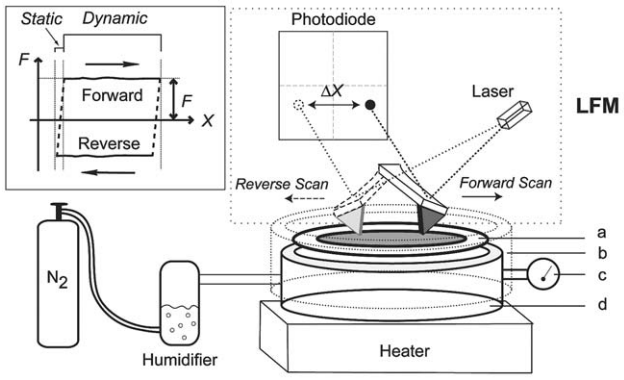

Fig. 2. F-LFM set-up: a combination of a LFM and a membrane chamber. The membrane chamber consists of (a) membrane sample on a copper ring support, (b) membrane chamber cap, (c) pressure gauge and (d) chamber base. The inset illustrates a *friction loop* in LFM.

the Nafion® membrane at elevated temperatures and pressures. The membrane was exposed to humid air prior to F-LFM experiments, and thus, was saturated with water. Within the nitrogen glove box, the membrane was exposed to a 94% RH (relative humidity) hydrated nitrogen gas stream at the upstream side, while the cantilever facing the downstream side experienced a relative humidity of less than 10% at ambient pressure and temperature.

2.2. Instrumentals

This study involved two scanning force microscopy analysis methods: (a) stationary shear modulation force microscopy [18] and (b) flux-lateral force microscopy [25,26]. While SM-FM is an established method for determining rheological transitions, F-LFM is a novel instrumental technique for nanoscale, in situ mass transport evaluations of membrane systems. Both instrumental approaches involve a stand-alone commercial scanning probe microscope (SPM) (*Explorer*, Veeco Instruments), and bar-shaped uncoated silicon cantilevers (Nanosensors™, normal spring constant of ~0.1 N/m, torsional spring constant ~80 N/m).

2.2.1. Shear modulation force microscopy

SM-FM is a non-scanning nanorheological method that is well suited for surface rheological studies involving thermally activated transitions or relaxations. It has been used for determining structural phase transitions in thin films, e.g., glass transitions [23,28,29]. SM-FM involves a nanometer-sharp SPM cantilever tip that is brought into contact with the sample surface, as sketched in Fig. 1 [18,29]. While a constant load is applied, the probing tip is laterally modulated by an input waveform from a function generator (SP830, Stanford Research Systems) with a "no-slip" nanometer amplitude, i.e., a small enough amplitude that guarantees no relative probe-sample slippage. The modulation response is analyzed using a two-channel lock-in amplifier (Model 8300, Perkin-Elmer) by comparing the response signal to the input signal. The response amplitude is a measure of the contact stiffness, k_c, and if expressed in a fully elastic limit $k_c = 8G^*a$, where G^* and a are the reduced shear modulus and the contact area, respectively [30]. By maintaining a stationary tip contact at a constant load, changes in the contact area occur due to creep. The experimental observable in SM-FM is the shear modulation response amplitude that reflects changes in normal and shear modulus of the material. The response amplitude is recorded and plotted as a function of the temperature. Thermally-activated transitions in the material, such as the glass transition, are determined from the "kink" in the response curve, as illustrated in Fig. 1. In this study, an applied load, F_A, of 79 ± 10 nN, modulation amplitudes on the order of nanometers, and a frequency range of 3.7–4.3 kHz were used. The sample temperature was increased stepwise by 1.0 °C using a temperature controller from MMR Technology (Model K-20). SM-FM experiments were conducted in a glove box under a dry nitrogen atmosphere with relative humidity below 10%. The SM-FM system temperature reading was calibrated with bulk polystyrene (PS) films (atactic polystyrene from Polymer Source, $M_W = 96.5$, $M_W/M_N = 1.04$) of thickness greater than 200 nm. The uncertainty of the temperature controller was found to be ±0.1 °C. A schematic of the SM-FM experimental set-up is provided in Fig. 1.

2.2.2. Flux-lateral force microscopy

In typical LFM experiments, the cantilever is scanned at a constant velocity over the sample surface while the torsional deflection of the lever is recorded [25]. Due to friction, forward and reverse scanning traces exhibit a hysteresis loop as sketched in the inset of Fig. 2. This is referred to in the literature as *friction loop* [25]. The friction loop, reflecting twice the value of the friction force, was recorded with an oscilloscope (Model 54624A, Agilent). Absolute friction forces were determined utilizing a *blind calibration* method (see Appendix A) [31]. It is with this microscopic lateral force technique that local permeate fluxes through membrane systems can be recorded. The F-LFM combines a membrane holding chamber with a LFM as sketched in Fig. 2. The recorded friction force deduced from the friction loop is found to be sensitive to the inlet gauge pressure of the permeate stream, as shown in Fig. 3 involving three flux calibration standard samples (MFI zeolite membranes, micropore sizes of ~0.5 nm [32]). The effluent nitrogen gas stream acts as a "gas lubricant" to the cantilever-sample contact. It has been experimentally ascertained that the friction force is a linear function of the gauge pressure, and its slope is a direct measure of the permeation flux. This is illustrated in Fig. 3 on MFI zeolite calibration standard samples. The deduced friction force–pressure gradient, m_k, from the $F(P)_k = -m_kP + b_k$ relationships in Fig. 3 ($k = 1$, 2 and 3 identifying the three calibration standard samples), provides a calibration factor of 13.1 N mol^{-1} s^{-1} m^{-2} when related to the conventionally determined permeabilities of the zeolite membranes, Fig. 3 inset. A reversed sign orientation of m_k was chosen to present the data in registry with nitrogen permeation changes. Conventional gas permeation experiments involved a vacuum system with a calibration receiving cylinder. The F-LFM analysis of the Nafion® membrane was conducted at membrane temperatures ranging between 22 and 95 °C, and a hydrated

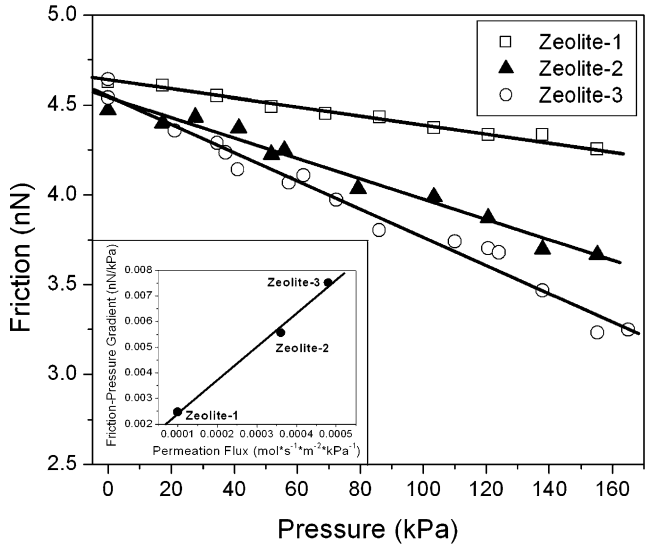

Fig. 3. F-LFM flux calibration: friction–pressure plots of calibration standards. *Inset*: the linear correlation between the conventionally measured permeability and the friction–pressure gradients, m_k, provides a flux calibration factor of 13.1 N mol^{-1} s^{-1} m^{-2}.

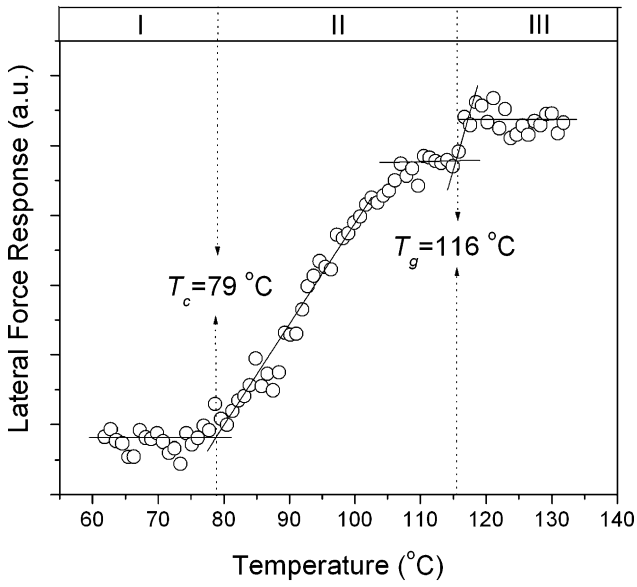

Fig. 4. SM-FM analysis of dehydrated Nafion® (EW of 1100) measured at 79 ± 10 nN applied load. Shear response forces reveal two transition temperatures that identify three regimes. Regime I and III reflect the glass state and the rubber melt state of Nafion®, respectively. Regime II encompasses the creep regime over which the cantilever sinks into the polymer matrix to equilibrate the contact pressure, and the saturation regime that defines the phase between the glass and rubber states.

nitrogen inlet gauge pressure of 5–60 kPa. To achieve steady conditions, lateral force measurements were recorded after 30 min following an increase of the inlet nitrogen pressure at each temperature, and 1 h after adjusting the membrane temperature. The friction measurements were performed over a 1 μm scan range at a velocity of 1 μm/s.

3. Results and discussion

A vacuum-annealed dehydrated thin Nafion® film on silicon was analyzed with SM-FM under dry nitrogen atmospheric conditions (RH < 10%). The objective was to investigate whether the solvent-free Nafion® matrix exhibited low-temperature reorganizations (relaxations) below the glass transition temperature. The shear response, in terms of a lateral deflection force, is plotted in Fig. 4 as a function of the temperature. Two distinct transition peaks are recognizable, one at 79 ± 1 °C and the other one at 116 ± 1 °C. The high-temperature transition value of 116 °C corresponds to the reported bulk glass transition temperature values of 110 °C [13]. At 79 °C, a significant reorganization of the material leads to a drop in the internal pressure of the material, similar to the glass transition. At such transitions, the cantilever tip sinks in until the contact area increases to a degree that the pressure is equilibrated. Typically, changes in the contact area dominate changes in the modulus in nano-experiments [23]. Due to the lack of contact area determination in SFM experiments of compliant materials, only forces but no pressures can be deduced.

The region between the low and high-temperature transitions, highlighted in Fig. 4 as region II, represents the creep regime, over which the internal pressure change is equilibrated in the contact zone of the probing tip by increasing the contact area. It is important to point out that below 79 °C thermally induced modifications of the contact zone can be neglected, as the contact stiffness remains constant.

As stated above, only a handful of studies have addressed the possibility of structural reorganizations in perfluorinated ionomer membranes at the critical operational temperature of ∼80 °C for fuel cell operation [16,33]. With F-LFM, we explored the impact of the structural reorganization at 79 °C on water transport in a commercial Nafion® 115 PEM membrane. The membrane was placed onto the airtight membrane holding chamber, Fig. 2, through which it was exposed to a hydrated nitrogen gas on the upstream side. The downstream side of the membrane, kept dry with nitrogen (<10% RH), nitrogen environment, was probed by a cantilever tip at a constant sliding velocity. From the friction loop, friction forces were determined as a function of the applied gas pressure and the applied cantilever probing-load over a temperature range of 22–95 °C. Fig. 5 shows representative friction–pressure relationships recorded at 75 °C, which is below the low-temperature relaxation of Nafion®, at two different cantilever loads. The slope of the friction–pressure plot, i.e., the friction–pressure gradient, is related to the amount of hydrated nitrogen gas permeation through the membrane. The friction force decreased as the inlet gas pressure increased, in accordance to the above discussed calibration on zeolite membranes. The friction–pressure gradient is a measure of the nitrogen permeability, as in the case of the zeolite membranes. The friction force, F, increased with the applied load according to Amonton's law ($F = \mu F_N$), where F_N is the normal load and μ is the friction coefficient.

Friction–pressure gradients as a function of the temperature, $m(T)$, of the Nafion® 115 PEM membrane are presented in Fig. 6a. Neither a qualitative nor an absolute dependence on

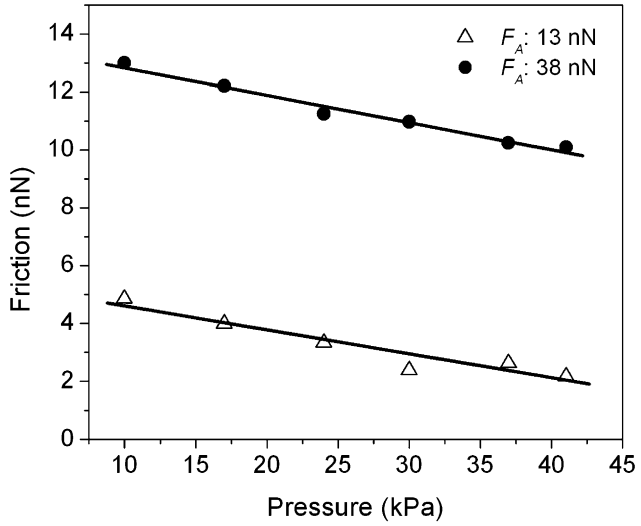

Fig. 5. Representative F-LFM analysis of hydrated nitrogen flow through a Nafion® 115 PEM membrane at 75 °C.

the probing load is observed. Up to a temperature of 70 °C, $m(T)$ increases steadily, as found for the permeability of nitrogen through Nafion® [10–12,34–36]. A significant increase in the transport properties is observed above 70 °C. Between 70 °C and the low-temperature matrix relaxation at 79 °C, discussed above with Fig. 4, two distinct signal responses occur in the $m(T)$ plots of Fig. 6a, highlighted in Fig. 6b, one belonging to the enhanced nitrogen transport and the other one to water transport. As there is not enough information available regarding the lubricating impact of neither nitrogen nor water, the two signals cannot be assigned unequivocally to either of the two fluids. Considering the steady extension of $m(T)$ from below 70 °C, it can be argued that the lower dotted trend line in the temperature interval between 70 and 79 °C represents the nitrogen flux, and the upper dotted-dashed trend line represents the onset of water transport in the Nafion® membrane. The data representation of the lower dotted trend line is improved at higher loads.

Above 79 °C, the sign of $m(T)$ was found to be reversed, indicating that the friction force increases with pressure. In this regime, the cantilever experiences a water-swollen membrane with masked nitrogen transport and dominant water transport. In contrast to the "incompliant" zeolite membrane, the Nafion® polymer membrane is elastically and plastically deformed by the tip, which exerts pressures in the contact zone on the order of 100 MPa [21]. Particularly plastic deformations can dominate any other source of frictional dissipation. Thus, as the qualitative behavior of $m(T)$ below 79 °C is a direct consequence of nitrogen and water permeation, above 79 °C $m(T)$ is dominated by the deformation properties of the swollen Nafion® membrane.

As in the case of any glass former, where the calorimetric glass transition can be understood as the "midpoint" temperature over which the transition occurs, we should also consider that the low-temperature transition at 79 °C is such a midpoint temperature. Hence, the 70 °C mark, at which the nitrogen and water transport is affected, can be inferred to be within the temperature regime over which the low-temperature relaxation in Nafion® occurs.

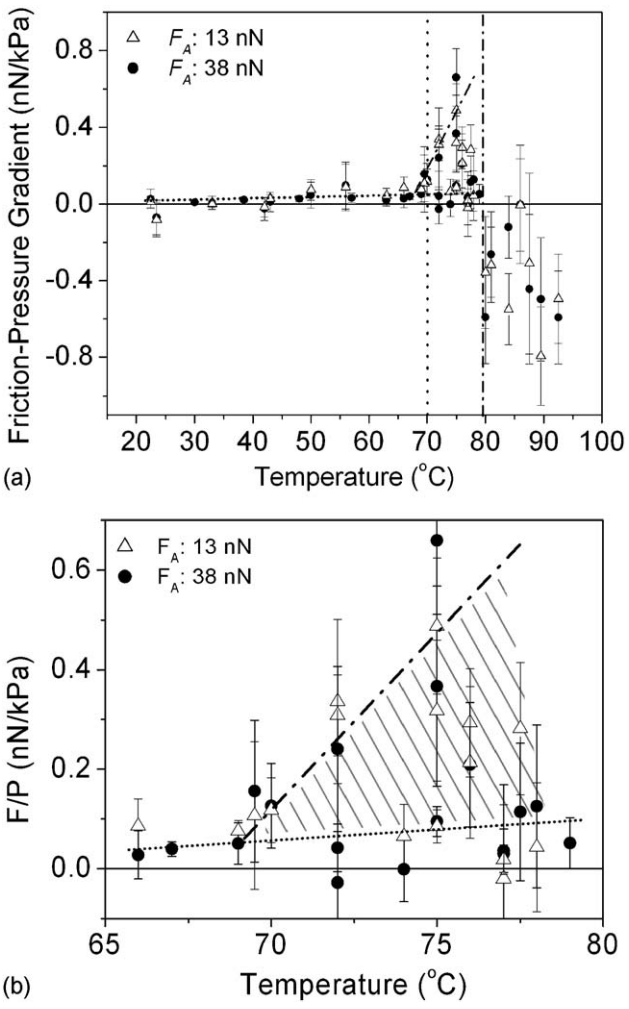

Fig. 6. (a) Friction–pressure gradients of the Nafion® 115 PEM membrane as a function of the temperature at applied loads of 13 nN (triangle) and 38 nN (dot). The regime up to the vertical dashed line at 70 °C reflects an increase in the nitrogen flux (visually enhanced by the dotted trend line). Nominally increased fluxes are observed above 70 °C, and below the low-temperature matrix relaxation of dehydrated Nafion® at 79 °C (indicated by the second vertical dashed line). Above the 79 °C mark, the force pressure gradient is reversed, reflecting the changes of the water-swollen PEM membrane. (b) Enlargement of the transition region where the onset of water transport is recognizable. Water and nitrogen transport occurs simultaneously as indicated by the shaded area. Two distinct signal responses occur in between 70 and 79 °C, indicative of the two transports of nitrogen (dotted line) and water (dotted-dashed line).

4. Conclusions

To obtain a fundamental understanding on the intricacy of structural relaxations within PEM membranes and mass transport properties of the membranes, it is necessary to study local fluid fluxes in parallel to relaxation properties. Nanoscopic methods of SM-FM and F-LFM were introduced for in situ analyses of local fluxes and structural relaxation properties. Rheological material relaxations in Nafion® were studied in conjunction with the water transport properties of Nafion® around its typical operation temperature of ~80 °C.

A structural transition at 79 °C, about 30–40 °C below the glass transition temperature of Nafion® (H^+ form), was found for

the dehydrated membrane. Local flux measurements of hydrated nitrogen show that water is trapped within the polymer membrane below the low-temperature structural transition, which explains the poor proton transport efficiency of the Nafion® perfluorinated ionomer membrane at temperatures below ∼80 °C.

It is important to note that the low-temperature structural transition at 79 °C was observed for the dehydrated membrane, and thus, is specific to the polymer matrix and not, as frequently assumed, a sole consequence of the kinetics of the solvent-containing aggregates within the apolar perfluorocarbon matrix. This is good news from an engineering perspective, as it is easier to control the polymer relaxation properties through appropriate molecular synthesis than to control the kinetics of such a complex solvent–polymer system. One of the remaining tasks is to pinpoint the molecular or submolecular origin for the low-temperature structural transition to obtain a handle for desired alterations in the molecular design of Nafion®.

We believe that the two introduced microscopic techniques (F-LFM and SM-FM) show great potential as "*local probes*" for studying the intricacy of flux and relaxation properties of modern heterogeneous composite materials used for organic electrolyte systems. Future tasks will involve the extension to other gaseous permeates such as oxygen, hydrogen and methane, but also liquid permeates such as methanol that are relevant fuel to cell technology.

Acknowledgments

We gratefully acknowledge Michael Tsapatsis from the University of Minnesota for providing us with MFI zeolite samples. This work was supported by the Petroleum Research Fund administered by the American Chemical Society, and the Royalty Research Fund of the University of Washington.

Appendix A

For a cantilever without reflecting coating, the *torsional geometry factor* of the cantilever Γ, linearly relating the lateral force

$$F_L = \Gamma \Delta I_L, \tag{A.1}$$

with the lateral photodiode signal, ΔI_L, is generally only in need of two parameters: the normal spring constant, k_N [31], and a torsional spring constant. The Young's modulus, E, and the density, ρ, of the cantilever material (silicon), and the cantilever length, l, and width, w, are typically provided by the manufacturer. The normal spring constant can be determined with an accuracy of ∼10% from resonance measurements using the following relationship [37,38]:

$$k_N = \frac{Ewt^3}{4l^3} \quad \text{with} \quad t = 6.190415\sqrt{\frac{\rho}{E}} f_1 l^2, \tag{A.2}$$

where t is the lever thickness and f_1 is the measured first resonance frequency in normal direction of the cantilever. In this study, the Young's modulus and density were 1.69×10^{11} N/m^2 and 2.33×10^3 kg/m^3, respectively.

The cantilever's lateral (i.e., torsional) spring constant is determined by means of friction comparison, utilizing the well-calibrated friction coefficient $\mu = 0.18 \pm 0.03$ (RH < 10%) between a silicon cantilever and a silicon calibration surface specifically prepared for this purpose (see below) [31]. The lateral force can be expressed as

$$F_L = \mu F_N = \Gamma \Delta I_L, \quad \text{with} \quad \Delta I_L = m_{cal} F_N, \tag{A.3}$$

where $F_N = k_N \Delta z$ (Δz normal deflection) is the normal force and m_{cal} is the ratio between the lateral force signal change and the normal force change. We refer to the experimentally determined m_{cal} as the *dimensional friction calibration factor*. As per Eq. (A.3), the torsional geometry factor, Γ, is given as the ratio of the friction coefficient μ and the experimentally determined calibration factor:

$$\Gamma = \frac{\mu}{m_{cal}}. \tag{A.4}$$

With the knowledge of Γ, the lateral photodiode signal can be directly converted into an absolute lateral force in Newtons, via Eq. (A.1).

Although not necessary here, sometimes it is desirable to know the lateral cantilever stiffness k_L, which is defined as

$$F_L = k_L \Delta x, \tag{A.5}$$

where Δx represents the lateral deflection distance. To obtain k_L, the sensitivity of the laser beam detection scheme has to be determined. Assuming that the sensitivity in the normal direction is the same as in lateral directions, the sensitivity factor, S, converts the photodiode signal, ΔI_N, into a normal distance, Δz. It is generally obtained from force displacement (FD) curves, provides the means to express F_L as

$$F_L = k_L S \Delta I_L. \tag{A.6}$$

Combined with Eq. (A.1), it follows:

$$k_L = \frac{\Gamma}{S}. \tag{A.7}$$

This *blind calibration* method strongly depends on a reliable reproduction of the surface that is used for the calibration. A hard silicon ⟨0 0 1⟩ surface is used as the calibration standard in our laboratory. The assumingly non-compliant silicon ⟨0 0 1⟩ surface is chemically treated to obtain a stable oxide surface, which should not be confused with stripping or hydrogen passivation techniques, e.g., HF treatments, which remove the surface oxide layer and render a very reactive surface, and thus, unstable. The procedure requires sequential sonication of the silicon calibration sample: first in acetone for 15 min, then in methanol for 30 min (HPLC grade from commercial sources). The sample is then rinsed with ultra-pure water. Finally, the silicon calibration standard is heated above 100 °C in a low humidity environment, preferably in a vacuum oven, to remove excess water. This procedure provides reproducible calibration samples for up to 2 h, depending on the post-treatment environmental conditions, i.e., relative humidity. Our calibration is generally obtained in a dry nitrogen environment (RH < 10%).

References

[1] H.L. Yeager, A. Eisenberg, Perfluorinated ionomer membranes, in: A. Eisenberg, H.L. Yeager (Eds.), ACS Symp. Series 180, Amer. Chem. Soc, Washington, DC, 1982.

[2] M.R. Tant, K.A. Mauritz, G.L. Wilkes, Ionomers: Synthesis, Structure, Properties and Applications, Blackie Acedemic and Professional, London, 1997.

[3] D.A. Mologin, P.G. Khalatur, A.R. Khokhlov, Molecular simulations of Nafion membranes in the presence of polar solvents, in: J. Samios, V.A. Durov (Eds.), Novel Approaches to the Structure and Dynamics of Liquids: Experiments, Theories and Simulations, Kluwer Academic, Boston, 2004.

[4] M. Rikukawa, K. Sanui, Proton-conducting polymer electrolyte membranes based on hydrocarbon polymers, Prog. Polym. Sci. 25 (2000) 1463–1502.

[5] T.A. Zawodzinski, J. Davey, J. Valerio, S. Gottesfeld, The water content dependence of electro-osmotic drag in proton-conducting polymer electrolytes, Electrochim. Acta 40 (1995) 297–302.

[6] X.M. Ren, W. Henderson, S. Gottesfeld, Electro-osmotic drag of water in ionomeric membranes, J. Electrochem. Soc. 144 (1997) L267–L270.

[7] J.J. Baschuk, X. Li, Modeling of polymer electrolyte membrane fuel cells with variable degrees of water flooding, J. Power Sources 86 (2000) 181–196.

[8] M. Fujimura, T. Hashimoto, H. Kawai, Small-angle X-ray-scattering study of perfluorinated ionomer membranes I origin of 2 scattering maxima, Macromolecules 14 (1981) 1309–1315.

[9] R.S. McLean, M. Doyle, B.B. Sauer, High-resolution imaging of ionic domains and crystal morphology in ionomers using AFM techniques, Macromolecules 33 (2000) 6541–6550.

[10] T. Sakai, H. Takenaka, E. Torikai, Gas-diffusion in the dried and hydrated Nafions, J. Electrochem. Soc. 133 (1986) 88–92.

[11] Z. Ogumi, T. Kuroe, Z. Takehara, Gas permeation in SPE method II. oxygen and hydrogen permeation through Nafion, J. Electrochem. Soc. 132 (1985) 2601–2605.

[12] K. Broka, P. Ekdunge, Oxygen and hydrogen permeation properties and water uptake of Nafion 117 membrane and recast film for PEM fuel cell, J. Appl. Electrochem. 27 (1997) 117–123.

[13] S.C. Yeo, A. Eisenberg, Physical-properties and supermolecular structure of perfluorinated ion-containing (Nafion) polymers, J. Appl. Polym. Sci. 21 (1977) 875–898.

[14] T. Takamatsu, A. Eisenberg, Densities and expansion coefficients of Nafion polymers, J. Appl. Polym. Sci. 24 (1979) 2221–2235.

[15] I.M. Hodge, A. Eisenberg, Dielectric and mechanical relaxations in a nafion precursor, Macromolecules 11 (1978) 289–293.

[16] A. Sen, K.E. Leach, R.D. Varjian, Determination of Water Content and Resistivity of Perfluorosulfonic Acid Fuel Cell Membranes, Materials Research Society, 1995, pp. 157–162.

[17] P.C. Riecke, N.E. Vanderborgh, Temperature-dependence of water-content and proton conductivity in polyperfluorosulfonic acid membranes, J. Membrane Sci 32 (1987) 313–328.

[18] R.M. Overney, C. Buenviaje, R. Luginbuehl, F. Dinelli, Glass and structural transitions measured at polymer surfaces on the nanoscale, J. Thermal Anal. Cal. 59 (2000) 205–225.

[19] G. Alberti, M. Casciola, Composite membranes for medium-temperature PEM fuel cells, Ann. Rev. Mater. Res. 33 (2003) 129–154.

[20] R.M. Overney, D.P. Leta, L.J. Fetters, Y. Liu, M.H. Rafailovich, J. Sokolov, Dewetting dynamics and nucleation of polymers observed by elastic and friction force microscopy, J. Vac. Sci. Technol. B 14 (1996) 1276–1279.

[21] C. Buenviaje, S. Ge, M. Rafailovich, J. Sokolov, J.M. Drake, R.M. Overney, Confined flow in polymer films at interfaces, Langmuir 15 (1999) 6446–6450.

[22] S.E. Sills, R.M. Overney, W. Chau, V.Y. Lee, R.D. Miller, J. Frommer, Interfacial glass transition profiles in ultrathin, spin cast polymer films, J. Chem. Phys. 120 (2004) 5334–5338.

[23] T. Gray, R.M. Overney, M. Haller, J. Luo, A.K.-Y. Jen, Low temperature relaxations and effects on poling efficiencies of dendronized non-linear optical side-chain polymers, Appl. Phys. Lett. 86 (2005) 211908.

[24] The equivalent weight (EW) is defined as the grams of polymer per mole of exchange sites, or the grams of the polymer in acid form that will neutralize one equivalent of base.

[25] R. Overney, E. Meyer, Tribological investigations using friction force microscopy, Mater. Res. Soc. Bull. 18 (1993) 26–34.

[26] R.M. Overney, Nanotribological studies on polymers, TRIP 3 (1995) 359–364.

[28] R. Luginbuhl, R.M. Overney, B.D. Ratner, Nanobiotribology at the confined biomaterial interface, in: ACS Symposium: Interfacial Properties on the Submicrometer Scale, 2001, pp. 178–196.

[29] S. Ge, Y. Pu, W. Zhang, M. Rafailovich, J. Sokolov, C. Buenviaje, R. Buckmaster, R.M. Overney, Shear modulation force microscopy study of near surface glass transition temperature, Phys. Rev. Lett. 85 (2000) 2340–2343.

[30] C. Buenviaje, F. Dinelli, R.M. Overney, Investigations of heterogeneous ultrathin blends using lateral force microscopy, Macromol. Symp. 167 (2001) 201–212.

[31] C.K. Buenviaje, S.R. Ge, M.H. Rafailovich, R.M. Overney, Atomic force microscopy calibration methods for lateral force, elasticity, and viscosity, Mater. Res. Soc. Symp. Proc. 552 (1998) 187–192.

[32] G. Xomeritakis, A. Gouzinis, S. Nair, T. Okubo, M. He, R.M. Overney, M. Tsapatsis, Growth, microstructure, and permeation properties of supported zeolite (MFI) films membranes prepared by secondary growth, Chem. Eng. Sci. 54 (1999) 3521–3531.

[33] P.C. Riecke, N.E. Vanderborgh, Temperature dependence of water content and proton conductivity in polyperfluorosulfonic acid membranes, J. Membrane Sci. 32 (1987) 313–328.

[34] Y. He, E.L. Cussler, Ammonia permeabilities of perfluorosulfonic membranes in various ionic forms, J. Membrane Sci. 68 (1992) 43–52.

[35] T. Sakai, H. Takenaka, N. Wakabayashi, Y. Kawami, E. Torikai, Gas permeation properties of solid polymer electrolyte (SPE) membranes, J. Electrochem. Soc. 132 (1985) 1328–1332.

[36] Y.T. Lee, K. Iwamoto, M. Seno, Gas permeabilities of perfluorocarboxylate membranes in various ionic forms, J. Membrane Sci. 49 (1990) 85–93.

[37] M. Nonnenmacher, J. Greschner, O. Wolter, R. Kassing, Scanning force microscopy with micromachined silicon sensors, J. Vac. Sci. Technol. B 9 (1991) 1358–1362.

[38] E. Meyer, R.M. Overney, Nanoscience—Friction and Rheology on the Nanometer Scale, World Scientific, NJ, 1998.